Hydrodynamics in a Gas-Solids Fluidized Bed Using X-Ray Fluoroscopy and Pressure Fluctuation Measurements

Bangyou Wu,[1,2] *Zhengxing He,*[1,2] *Apostolos Kantzas,**[1,2] *Céline T. Bellehumeur,*[2] *Sergey Kryuchkov*[1,2]

Summary: In this work, non-intrusive techniques were used to characterize the hydrodynamics in a gas-solids bubbling fluidized bed using polyethylene powder and glass beads of comparable mean diameter ($d_p = 360$ μm) but different density. X-ray fluoroscopy measurements and pressure fluctuations were performed on a pseudo 2-dimensional gas-solids fluidized bed. Bubble properties were captured from X-ray fluoroscopy measurements. Similarities and differences of flow behavior of the two particle systems were revealed from comparison of bubble properties. Bubble properities normally varied similary with operating conditions for the two particle systems, while bubble sizes for the glass beads system are larger than those for the polyethylene system. Wavelet analysis of pressure fluctuations was applied to investigate the gas and solids phase flow behavior. Multi-scale flow behavior was extracted from the standard deviation of the decomposed coefficient series. Flow behavior due to particles and bubbles of different sizes were captured at different decomposition levels of pressure fluctuations, which is difficult to know from analysis of the original signal. Results extracted from X-ray fluoroscopy and pressure fluctuation measurements were consistent, suggesting that conventional pressure fluctuation measurements can be effectively used for investigation of the bubbling behavior.

Keywords: cycle time; fluidized bed; polyethylene; wavelet analysis; X-ray fluoroscopy

Introduction

Gas-phase fluidized bed reactors are used in a wide range of applications in refining, upgrading, pharmaceutical, food and chemical industry. The production of polyolefins is one important example of such applications. The modeling of the performance of fluidized bed polymerization reactors is complex and requires the consideration of mass and energy transfer at the macroscale level, intra and inter particle mass and energy transfer, particle growth, particle interactions, and kinetics of polymerization. Ultimately, realistic hydrodynamic models are necessary for the design, scale-up, operation optimization and assessment of existing and new polymerization processes. Bubbling flow plays a key role in the hydrodynamic behavior, as it causes the motion and mixing of gas and solids phase. Many design parameters, the calculation of mass and heat transfer coefficient, and validation of computational fluid dynamic models require the information on bubble properties.[1] Most of published fluidized bed hydrodynamic behavior was based on experimental results for non-porous, solid particles. It is necessary to investigate the hydrodynamics using porous polyolefin power and compare with the results from non-porous particles.

[1] Tomographic Imaging and Porous Media Laboratory
E-mail: akantzas@ucalgary.ca
Tel.: +1-403-220-8907;
Fax: +1-403-282-5060
[2] Department of Chemical and Petroleum Engineering Schulich School of Engineering University of Calgary, Calgary, AB, Canada T2N 1N4

A broad range of techniques have been proposed to monitor hydrodynamic characteristics of fluidized beds, each with advantages and limitations. Among those, x-ray fluoroscopy allows for very fast tracking of image time series and can be used to visualize and capture the images from fluidized bed reactors.[1,2] However, continuous monitoring of pressure fluctuations in a bubbling fluidized bed is by far more feasible for real-time monitoring and control of the fluidization operations. Since pressure fluctuations in bubbling fluidized beds are mainly due to the gas phase flow behavior in the bubbling fluidized bed reactor, it is possible to investigate the bubbling behavior from pressure fluctuation measurement.[3,4]

It is widely accepted that multi-scale flow is a common characteristic in multiphase fluidized bed reactors.[5] Wavelet multiresolution analysis has gained significant attention for investigating the multiscale flow behavior in fluidized beds, as summerized by Wu *et al.*.[6] Wavelets are a family of functions of constant shape and zero mean that are localized in both the frequency and time domains. An original signal can be decomposed into many lower resolution components. Each level of decomposition contains information associated with a scale. A pseudo-frequency can be associated to a given scale.[7] The quality of signal decompositions and reconstruction mainly depends on the choice of the mother wavelet.[8] After decomposition, high-scale and low-frequency components of the signal are called approximations (A), and low-scale and high-frequency components of the signal are called details (D).

In the investigation of flow dynamics in fluidized beds and multi-phase flow using wavelet analysis, the selection of mother wavelets varies considerably from one study to another. The selected wavelet should well represent the characteristics of original signals, and therefore also depends on the type of probe and sampling parameters. In this study, Daubechies wavelet (DB6) has been chosen for the analysis of experimental data. Daubechies wavelet has a highest number of vanishing moments for a given support width and smoothness compared to blockier Haar wavelet,[7,9,10] ensuring that the signal analysis becomes more precise with the higher order of polynomials used for approximation. The number of vanishing moments of the wavelet dictates the detectable range of singularities. Matlab^{TM} with wavelet toolbox was used for signal process in this work.

In this study, pressure fluctuations and images of gas-solids flow for glass beads and polyethylene particle systems at ambient conditions were measured. The gas-solids flow behavior of polyethylene particle system was compared with that of glass beads particle systems. Results from X-ray fluoroscopy measurements were compared with those from pressure fluctuation measurements.

Experimental

The fluidized bed system consisted in a pseudo 2-D column made of Plexiglas with an inner width and thickness of 22.5 cm and 5 cm, respectively, the height of the fluidization section being 150 cm. A porous plate distributor was installed on the bottom of the column, and the gas entered the column through a cone at the bottom of an approximately 15 cm long chamber. The cone was filled with small plastic spheres (diameter = 6.35 mm) and the chamber was empty to improve the gas distribution before reaching the distributor. Valves and rotameters were used to adjust and measure the gas flow rate, respectively.

Two types of particles were tested glass-beads and polyethylene particle, with the column being filled with particles to a static bed height of 40 cm. Both particle systems had similar mean particle size (360 μm) and particle size distribution (297 −420 μm), while they differed in density (2480 kg/m^3 for glass-beads and 924 kg/m^3 for polyethylene particle). It should be noted that the polyethylene resins are porous particles. The value of 0.924 is plaque density that will be used in

the voidage calculation. The particle density and particle voidage are 0.613 g/cm^3 and 0.337, respectively. Both types of particles are classified as Geldart ''B''. The minimum fluidization velocity (U_{mf}) was determined by measuring the bed pressure at different velocities, and was found to be 11.0 cm/s for the glass-beads and 4.3 cm/s for the polyethylene particle. Three superficial gas velocities (U_g) were tested for each type of particles.

Four pressure transducers (Schlumberger Solartron, model 8000 DPD) were connected to four column wall pressure ports located at a height $h = 6$, 16, 36, and 56 cm above the distributor using 0.32 cm nylon tubes. An A/D converter, a PC-LPM-16 card from National Instruments, and a personal computer were used for data acquisition. A self-developed Labview^{TM} program records voltage data and stores them into the computer hard disc. The pressure data was collected at a rate of 500 Hz for 60 seconds at each flow rate. Each operating condition was sampled 20 times. Transducers were calibrated to establish the relationship of pressure versus voltage prior to the experimental measurements.

The X-ray fluoroscopy system (Figure 1) consisted of the X-ray tube, X-ray detector, image intensifier and image acquisition computer. The X-ray tube generated continuous X-rays by energy conversion when a stream of electrons produced at the cathode collides with a target or anode. The X-ray detector received the attenuated X-rays passing through the object to be imaged and converted the X-ray photons to electrical signals. The image intensifier enhanced the electrical signals, and converted them to a digital grayscale image. The image acquisition computer grabed the image at the rate of 30 frames per second and stored it to the hard disc. The grayscale number was correlated to bed voidage by calibration. Since the effective diameter of the image was some 17 cm, the size of the image was less than the width of the column. In this research, six parts of the column were imaged at each given superficial gas velocity. For each part, approximately 2 minutes worth of images were collected which amounted to 3600 frames. Additional details about the experimental setup and procedure can be found in reference.[11]

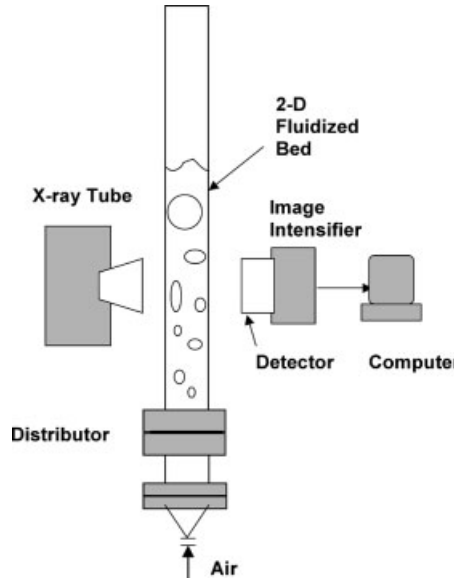

Figure 1.
Schematic of the X-ray fluoroscopy setup.

Results and Discussion

Wavelet based denoising methods by Roy *et al.*[12] were applied to the experimental pressure measurements. In this method, by differentiation of measured time series, contribution due to white noise moves toward the finer scales and this process distributes more energy to finer scales. Scalewise power versus scale (1-14) was first plotted. Thresholding scale level was identified as 2, therefore wavelet coefficients of scales 1 and 2 were set to be zero in the reconstruction of the denoised pressure fluctuation signal. The high frequency components were successfully removed after wavelet denoise.

Neighborhood averaging scheme was applied to the X-ray fluoroscopy images to remove noise. A global threshold of

grayscale number was used to determine the bubble boundary and binarize the grayscale images. A Matlab™ program was written to identify and track bubbles. The contrast between bubble and emulsion phase was found to be better for glass beads compared to polyethylene powder system. The grayscale number of the image varies from 0 (black) to 255 (white). Ideally, a bubble would be defined as a region without particles in the gas-solid fluidized bed. The application of this definition to determine the boundary of bubbles from images would lead to unreasonable results, because the bed was only pseudo 2-dimensional (thickness = 5 cm) and the bubbles normally had a cloud layer. In this research, the average value of maximum grayscale number of a large bubble and mean grayscale number of emulsion phase were selected as threshold used to determine the boundary of the bubble. We established the grayscale numbers for emulsion phase of glass beads system and polyethylene system to be approximately 71 and 115, respectively; the ideal grayscale numbers for bubbles were 230 for glass beads and 145 for polyethylene system. While variations in the selected threshold affected the bubble properties, the general trends of the profiles in the figures in this work estimated from X-ray fluoroscopy images remained unchanged. Furthermore, our results were compared with those obtained when using a local threshold method and no significant differences in the bubble properties were detected for bed height greater than 9 cm and bubble diameter larger than 2 cm.

Characterization of Gas-Solids Flow Behavior

Experimental results showed, as expected, that average pressure decreases with an increase of distance from distributor or a decrease of superficial gas velocity. The reduction in the average pressure was more significant in the bottom part of the bed ($h = 6$–16 cm), and was attributed to the initial acceleration of the particles.

Average cycle time (*ACT*) was used to characterize the average time interval of non-periodic pressure fluctuation. *ACT* is calculated using equation as follows:[13,14]

$$ACT = \frac{Total\ time}{(Number\ of\ crossing\ with\ the\ average)/2}$$

ACT was determined from pressure data and results are shown in Figure 2. *ACT* varies similarly with operating conditions for glass beads and polyethylene. *ACT* for glass beads being much higher than that of polyethylene under similar operating conditions. This result suggests that bubbles formed using glass beads (GB) are much larger than those for polyethylene particle (PE). This was verified from X-ray fluoroscopy measurements (Figure 3). The gas distribution for polyethylene would therefore be more uniform with low *ACT*, and may enhance the heat and mass transfer in fluidized bed reactors. *ACT* increases with an increase of U_g, which means less frequent and usually larger pressure fluctuations, caused by the formation of bubbles with large diameter (Figure 3), become dominant at higher U_g. This can be directly viewed from pressure time series at different U_g (Figure 4). This phenomenon is similar at different axial positions of the column and similar for both glass beads and polyethylene particles. The cyclic pressure fluctuations are strongly related to the bubbling behavior. Some researchers have correlated bubble properties, such as bubble diameter, to spectral analysis of pressure fluctuations.[3,4]

ACT is very low at $h = 56$ cm, which means that the pressure fluctuations at this position have low amplitude and high frequency. The static bed height is only 40 cm. At $h = 56$ cm, the solids phase is very dilute and the pressure fluctuation is mainly due to gas phase and bubble breakage at the top of the dense bed, therefore the fluctuation is weak and frequent with low *ACT*. *ACT* at $h < 36$ cm (Figure 2) does not vary significantly with bed height, the only exception being the *ACT* profile obtained for PE

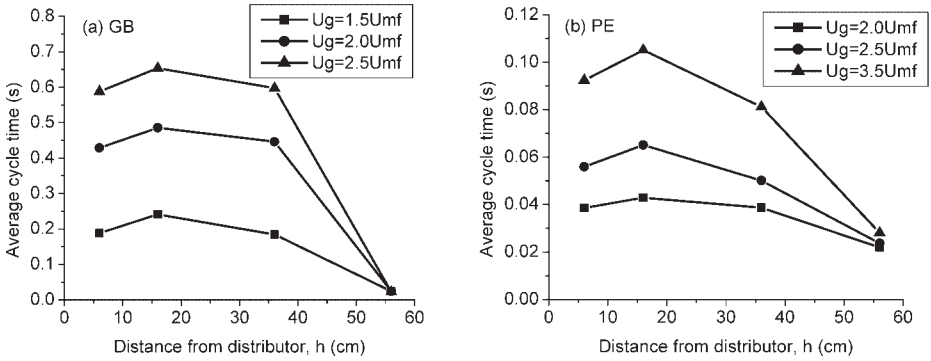

Figure 2.
Average cycle time for glass beads (GB) and polyethylene powder (PE).

particle at high U_g. Relatively higher *ACT* at $h = 16$ cm is likely caused by strong bubble interaction, such as bubble coalescence. As pressure fluctuations mainly reflect the global gas-solids flow behavior, it is difficult to distinguish the bubbling behavior at different bed positions from pressure fluctuations (Figure 5). In this work, bubble properties along the axial of column were extracted from X-ray fluoroscopy measurements.

Characterization of Multiscale Flow Behavior

Signal series were generally decomposed into approximations and details of different scales. Three levels of scales were considered to be sufficient representation of the flow dynamics in the fluidized bed systems:[15,16] micro-scale signals characterizing particle movement in clusters or in the dilute phase, meso-scale signals describing cluster behavior or their interaction with dilute phase, and macro-scale accounting for the effect of the unit on the system behavior. Each level of information decomposed by wavelet represents information of different frequency band of original signals.[17] The idea of three major scales was adopted in this study with different representations. Examples of decomposition of pressure fluctuations are shown in Figures 6 and 7.

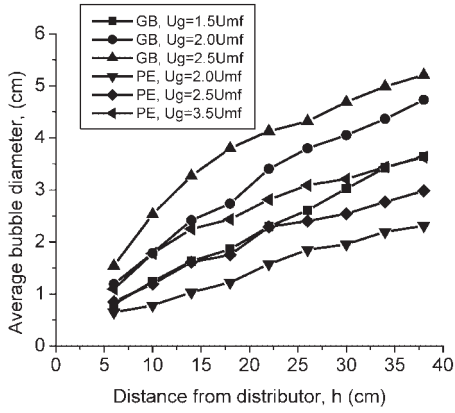

Figure 3.
Average bubble diameter as a function of distance from distributor.

As expected, Figures 6 and 7 show less high-frequency components in the approximations and detail series with an increase of scale. Fluctuation is very chaotic with mainly high-frequency and low-amplitude components for D1-D3, while there are more relatively large and smooth fluctuations in D4-D6. The approximate series A4-A6 show less small-scale fluctuation and A6 was used for further analysis of global bubbling behavior (macro-scale).

Average cycle time was calculated from approximate series at scale 6 (A6) providing information about the global bubbling behavior, as shown in Figure 8. *ACT* of A6 is much higher than that from original series (Figure 2) due to the clean and smooth nature of large-scale approximate series. In contrast to the trend shown in Figure 2(a)

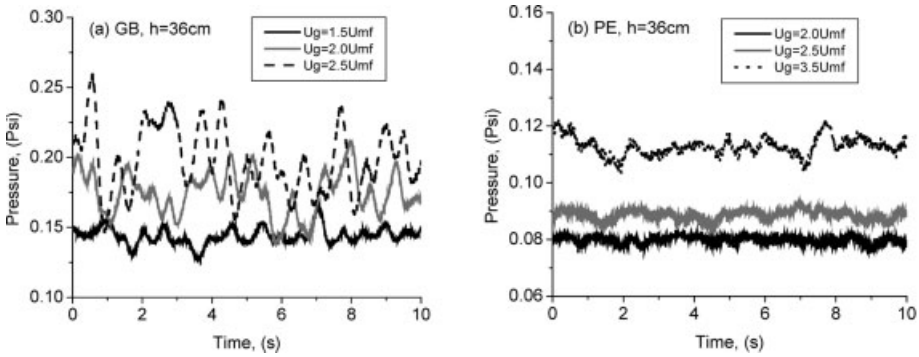

Figure 4.
Pressure time series at different superficial gas velocities.

using the original series for glass beads, *ACT* generated from A6 decreases with an increase of U_g at $h < 36$ cm. Most of small fluctuations with high frequency and low amplitude in the original series at lower U_g were removed in A6, the remaining series reflecting the time interval of appearance of large bubbles. A large *ACT* indicates the contribution of less frequent and larger bubbles to the original pressure fluctuation. For polyethylene particle, *ACT* from A6 varies with bed height and shows similar trends. *ACT* from A6 does not show important change with U_g, compared to that seen with the original series (Figure 2b). This suggests that the appearance frequency of large bubbles does not increase significantly with an increase of U_g. There must be many small and medium size bubbles, which make the uniform gas distribution in gas-polyethylene fluidized beds. Bubble diameter distribution as a

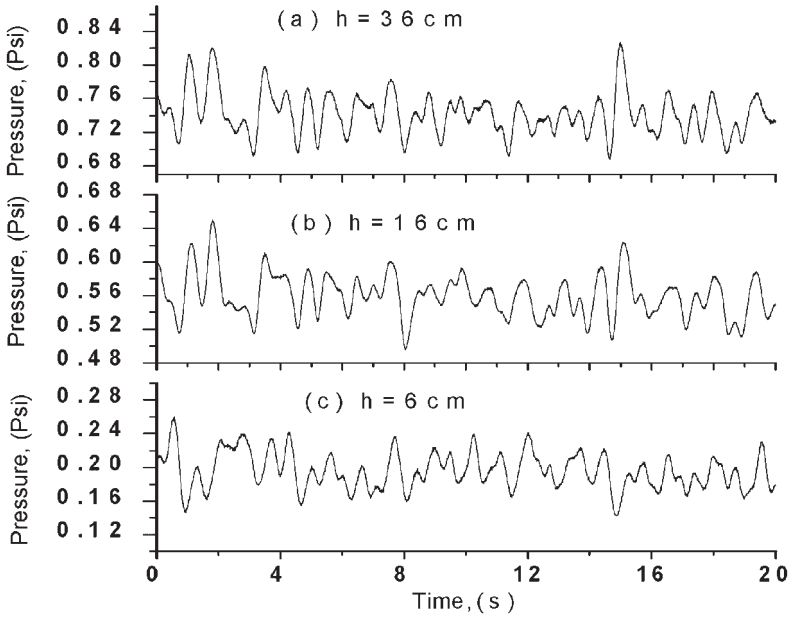

Figure 5.
Pressure time series at different bed height for glass beads at $U_g = 2U_{mf}$.

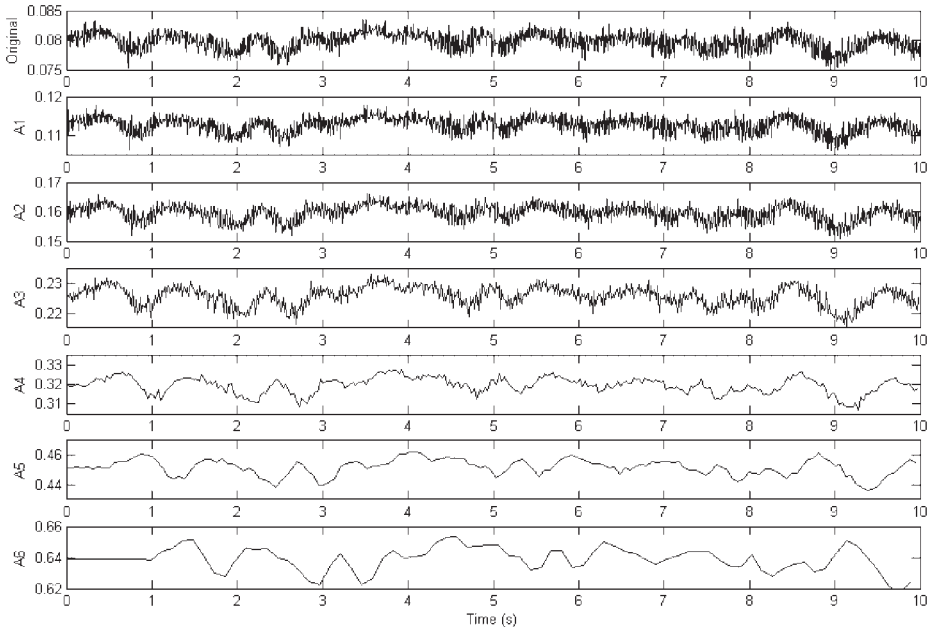

Figure 6.
Original pressure series and approximate coefficients series of scale 1-6 at $U_g = 2U_{mf}$ and $h = 36$ cm for polyethylene particles.

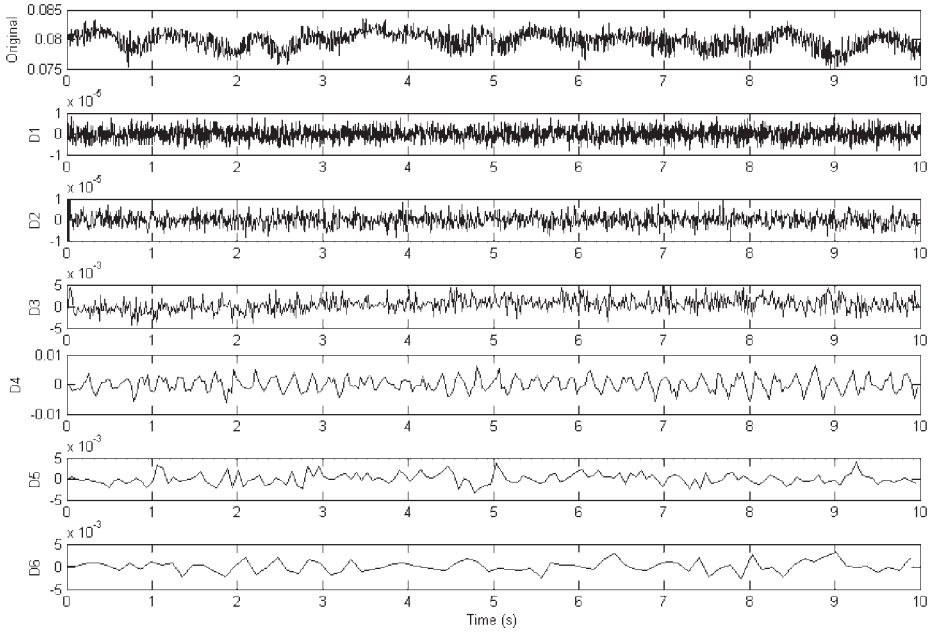

Figure 7.
Original pressure series and detail coefficients series of scale 1-6 at $U_g = 2U_{mf}$ and $h = 36$ cm for polyethylene particles.

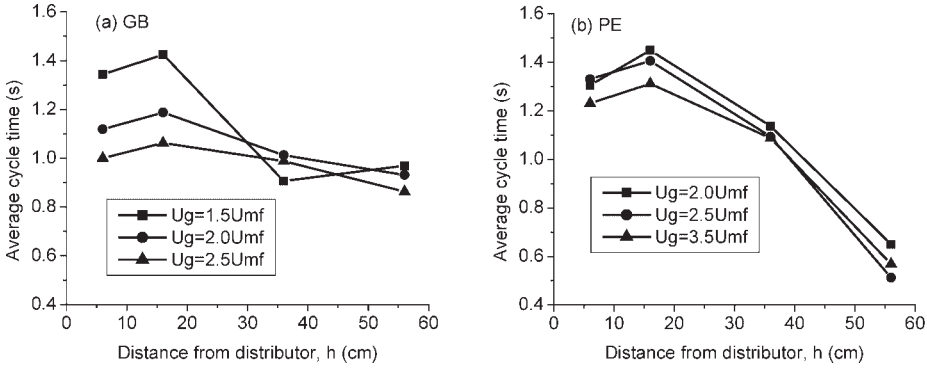

Figure 8.
Average cycle time for approximate coefficients of scale 6 (A6) for glass beads and polyethylene particle.

function of bubble diameter and superficial gas velocity is shown in Figure 9, which was obtained by processing of X-ray fluoroscopy images. Under comparable operating conditions, there is a larger fraction of small bubbles for polyethylene particles systems.

Analysis performed on global scale behavior (Figure 8b) suggest that bubbling behavior for PE particle is not significantly affected by gas velocity but only height. However, this is only for large bubbles, as fluctuation from A6 is only for large scale behavior. From Figure 9, bubble number fraction of large bubbles do not change significantly with superficial gas velocities. On the other hand, results obtained from analysing the original pressure signal (Figure 2b) suggest a dependence with gas velocity, which is the result of bubbles of all sizes.

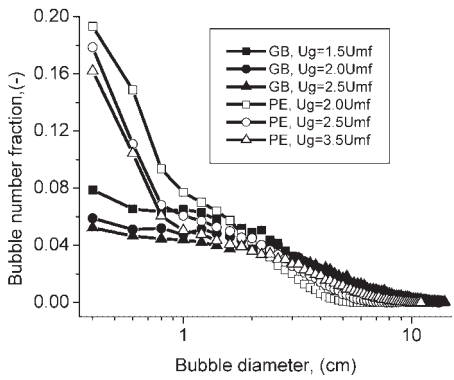

Figure 9.
Bubble diameter distribution at different superficial gas velocities.

In order to further quantify the difference among D1-D6, standard deviation (SD) was estimated from detail coefficients for both glass beads and polyethylene particles (Figure 10). SD from D1 and D2 are almost the same and close to zero. This confirms that D1 and D2 may be caused by micro-scale behavior of particles or electronic noise. As profile for D3-D6 changes with measurement positions, D3-D6 indicates certain amount of local behavior. Variation of SD with measurement positions is very significant for D3 and D4, indicating strong local behavior of meso-scale bubbles. D5 is likely caused by the combination of local and global meso-scale bubble behavior. Standard deviation estimated from D6 varied significantly with measurement positions for glass beads but much less significantly for polyethylene power. This indicated that glass beads are more likely to form large bubbles than polyethylene particles. Large bubbles also caused strong local behavior at scale 6 for glass beads. Larger bubble size for glass beads compared to polyethylene under comparable operation conditions was verified from X-ray fluoroscopy measurements (Figure 3). This indicated that bubble behavior could essentially be captured by pressure fluctuation measurement.

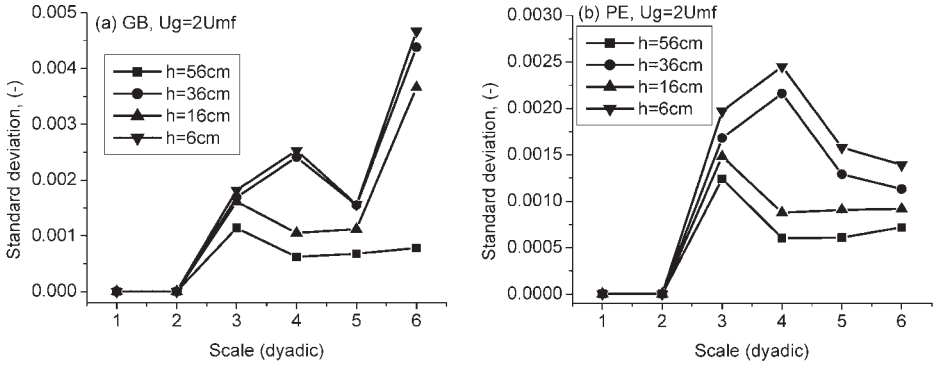

Figure 10.
Standard deviation estimated from detail coefficient series (D1-D6) decomposed from denoised pressure fluctuation for glass beads and polyethylene particle at $U_g = 2U_{mf}$.

Pressure measurements can be reliably used for monitor and control the flow behavior inside fluidized bed reactor.

Comparison of Experimental Bubble Properties and Correlation

Comparison of experimental and predicted bubble diameters at $U_g = 2.5U_{mf}$ is shown in Figure 11. The average bubble diameter varies with the axial bed position as well as with the type of particle system considered, which is captured by both experimental measurement and prediction from correlations. For both particle systems, the experimental bubble diameter is lower than the value predicted by the correlation of Mori and Wen[18] and Werther.[19] Our results do not show as good a match to the correlations as in Hulme and Kantzas.[1] This is likely due to the 2-D column used in this study with strong wall effect and non-spherical properties of the large bubbles (>5 cm) formed in the bed. While the two-dimensional column is a convenient tool to visualize the bubbling behavior of fluidized beds, our experimental observations show a poor match to the bubble properties predicted using published correlations.

Figure 12 presents a comparison between our experimental observations and predictions obtained from correlations proposed by Davidson and Harrison[20] and Kunii and Levenspiel.[21] The correlations predict an initial increase followed by a decrease in the velocity, a profile which is

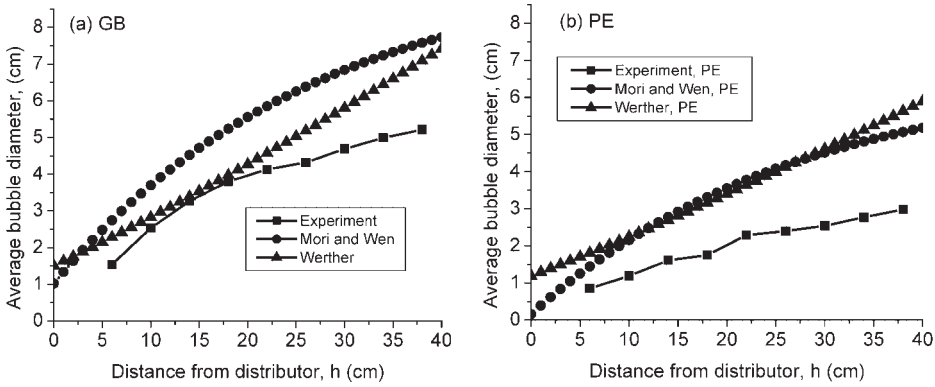

Figure 11.
Average bubble diameter as a function of distance from distributor at $U_g = 2.5U_{mf}$.

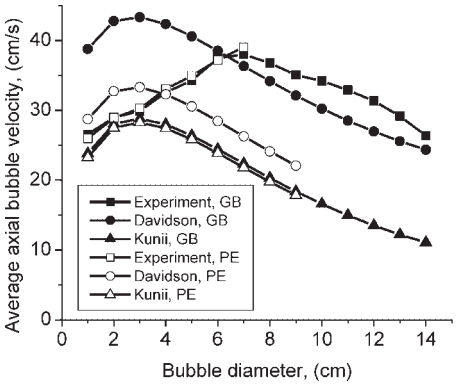

Figure 12.
Average axial bubble rise velocity as a function of distance from distributor.

associated with the change in the bubble size with the bed height. Experimental results obtained from x-ray fluoroscopy, on the other hand, showed that the bubble velocity only slightly increases with the axial bed position and nearly unaffected by the superficial gas velocity.[11] The differences between experimental observations and predictions for the bubble velocities are significant. Again, these differences may be due to a strong wall effect in the experimental measurement which is not taken into consideration in the estimation of hydraulic diameter from published correlations. Experimental measurements obtained from cylindrical columns showed a better comparison with published correlations and thus would be of better use for scale up of operation.

Conclusions

Wavelet denoising was effectively used for pretreatment of experimental pressure fluctuation measurements. The similarities and differences of flow dynamics between glass beads and polyethylene particle were identified using *ACT* from denoised pressure series. Multiscale flow behavior was further characterized from wavelet decomposition of denoised time series: Global (macro-scale) bubbling flow behavior was represented from A6; D1 and D2 were likely due to micro-scale flow behavior of particles or noise; D3-D6 reflected local meso-scale bubbling behavior. Glass beads are more likely to form large bubbles with strong local behavior compared to polyethylene under comparable operation conditions. Similarities and difference of bubbling behavior at different scales for glass beads and polyethylene particle systems from pressure fluctuations were verified from X-ray fluoroscopy measurements.

Bubble properties, such as bubble diameter and bubble velocity, were extracted from X-ray fluoroscopy measurements. Eventhough results from pressure fluctuation and X-ray fluoroscopy measurements were consistent, bubble properties from X-ray fluoroscopy measurements are not consistent with prediction from published correlations. This may be due to the 2-D feature of the column. Nevertheless, the results extracted from our analysis can further be used for the control of the flow dynamics in gas-phase polymerization reactors through pressure measurements. Our results will also facilitate the formulation and implementation of models, which account for variations in the properties of the granular solids, in the improvement of computational fluid dynamic (CFD) simulations of gas-solid fluidized bed systems.

Acknowledgements: Financial support from the Natural Science and Engineering Research Council of Canada and the Canada Research Chairs Program is gratefully acknowledged.

[1] I. Hulme, A. Kantzas, *Powder. Technol.*, **2004**, *147*, 20.
[2] A. Kantzas, I. Wright, A. Bhargava, F. Li, K. Hamilton, *Catalysis today*, **2001**, *64*, 189.
[3] J. Van der Schaaf, J.C. Schouten, F. Johnsson, C.M. van den Bleek, *Int. J. Multiphase Flow*, **2002**, *28*, 865.
[4] L. Van der Lee, B. Chandrasekaran, I. Hulme, A. Kantzas, *Can. J. Chem. Eng.*, **2004**, *82*, 220.
[5] J. Li, M. Kwauk, E, *Chem. Eng. Sci.*, **2003**, *58*, 521.
[6] B.Y. Wu, A. Kantzas, C. Bellehumeur, S. Kryuchkov, in: "*5th World Congress on Particle Technology*", conference proceding CD, **2006**.
[7] L.A. Briens, N. Ellis, *Chem. Eng. Sci.*, **2005**, *60*, 6094.
[8] M.C. Shou, L.P. Leu, *J. Chem. Eng. Japan*, **2005**, *38*, 409.

[9] N. Ellis, L.A. Briens, J.R. Grace, H.T. Bi, C.J. Lim, *Chem. Eng. J.*, **2003**, *96*, 105.
[10] N. Ellis, H.T. Bi, C.J. Lim, J.R. Grace, *Chem. Eng. Sci.*, **2004**, *59*, 1841.
[11] Z.X. He, M.Sc. Thesis, University of Calgary, Calgary, Canada, **2005**.
[12] M. Roy, V.R. Kumar, B.D. Kulkarni, J. Sanderson, M. Rhodes, M. vander Stappen, *AIChE J.*, **1999**, *45*, 2461.
[13] M.L.M. vander Stappen, Ph.D. Thesis, Delft University of Technology, Netherlands, 1996.
[14] L.A. Briens, Ph.D. Thesis, The University of Western Ontario, London, Canada, 2000.
[15] J.Q. Ren, J.H. Li, In: ''*Fluidization IX*'', L.S. Fan and T. M. Knowlton (eds), 1998, p. 629.
[16] J.Q. Ren, Q.M. Mao, J.H. Li, W.G. Lin, *Chem. Eng. Sci.*, **2001**, *56*, 981.
[17] G.B. Zhao, Y.R. Yang, *AIChE J.*, **2003**, *49*, 869.
[18] S. Mori, C.Y. Wen, *AIChE J.*, **1975**, *21*, 109.
[19] J. Werther, J.F. Davidson, D.L. Keairns, in: ''*Fluidization*'', Cambridge University Press, London, 1978, p.7.
[20] J. F. Davidson, D. Harrison, ''*Fluidized Particles*'', Cambridge University Press, New York, 1963.
[21] D. Kunii, O. Levenspiel, ''*Fluidization Engineering*'', 2nd edition.Butterworth-Heinemann, Boston, 1991.

